Journal of Cerebral Blood Flow & Metabolism (2015) 35, 1937–1949

www.jcbfm.com

ORIGINAL ARTICLE

CDK5 knockdown prevents hippocampal degeneration and cognitive dysfunction produced by cerebral ischemia

Johana A Gutiérrez-Vargas[1], Alejandro Múnera[2] and Gloria P Cardona-Gómez[1]

Acute ischemic stroke is a cerebrovascular accident and it is the most common cause of physical disabilities around the globe. Patients may present with repeated ictuses, experiencing mental consequences, such as depression and cognitive disorders. Cyclin-dependent kinase 5 (CDK5) is a kinase that is involved in neurotransmission and plasticity, but its dysregulation contributes to cognitive disorders and dementia. Gene therapy targeting CDK5 was administered to the right hippocampus of ischemic rats during transient cerebral middle artery occlusion. Physiologic parameters (blood pressure, pH, pO_2, and pCO_2) were measured. The CDK5 downregulation resulted in neurologic and motor improvement during the first week after ischemia. Cyclin-dependent kinase 5 RNA interference (RNAi) prevented dysfunctions in learning, memory, and reversal learning at 1 month after ischemia. These observations were supported by the prevention of neuronal loss, the reduction of microtubule-associated protein 2 (MAP2) immunoreactivity, and a decrease in astroglial and microglia hyperreactivities and tauopathy. Additionally, CDK5 silencing led to an increase in the expression of brain-derived neurotrophic factor (BDNF), its Tropomyosin Receptor kinase B (TRKB) receptor, and activation of cyclic AMP response element-binding protein (CREB) and extracellular signal-regulated kinase (ERK), which are important targets in neuronal plasticity. Together, our findings suggest that gene therapy based on CDK5 silencing prevents cerebral ischemia-induced neurodegeneration and motor and cognitive deficits.

Journal of Cerebral Blood Flow & Metabolism (2015) **35,** 1937–1949; doi:10.1038/jcbfm.2015.150; published online 24 June 2015

Keywords: CDK5 RNAi; cerebral ischemia; cognitive disorder; gene therapy; neuroprotection

INTRODUCTION

Stroke is responsible for more than 5 million deaths each year worldwide, making it the second leading cause of death and a major cause of disability.[1] In Latin America, stroke is the consequence of metabolic disorders and life style. Thrombolytic therapy is the only approved treatment for acute ischemic stroke.[2] However, the restoration of blood flow after thrombolytic treatment may aggravate the initial injury and lead to a secondary injury known as ischemia/reperfusion (I/R) injury.[3] Currently, there is no gold standard treatment outside the thrombolytic therapeutic window that prevents long-term physical and mental disabilities after stroke. Neuroprotective agents against ischemia have been proposed for decades, and promising newer stroke treatments have been developed in animal models, but their efficacies in patients remain limited.[4] Hence, there is an urgent need to develop effective neuroprotective strategies to prevent progressive cerebral impairment after stroke.

Cognitive disorders and vascular dementia are 25% more prevalent during the first year after stroke.[5] Tau hyperphosphorylation is considered as a neurodegeneration hallmark after cerebral ischemia and is strongly correlated with cognitive disorders and dementia. Cyclin-dependent kinase 5 (CDK5) has been considered as a major tau kinase that contributes to tau pathology in cerebral ischemia.[6] Cdk5 is a proline-directed serine/threonine kinase that is ubiquitous in the nervous system, playing important roles in synaptic plasticity and neurotransmission; in addition, its overregulation is involved in neurodegeneration.[7] The CDK5 activity in the brain is triggered by its binding partners, p39 and p35.[8] During excitotoxic processes and subsequent disruption of calcium homeostasis in cerebral ischemia, the conversion of p35 to p25 is mediated via proteolytic cleavage by the calcium-regulated protein calpain. The p25 fragment triggers CDK5 hyperactivation and translocation of the p25/CDK5 complex to the cytoplasm, promoting the phosphorylation of tau at specific epitopes, a prerequisite of paired helical filament (PHF) formation and leading to neuronal death.[6] Several classes of potent inhibitors for CDK5 have been described[9] and have been shown to have neuroprotective potential in cerebral ischemia.[10] However, most of these inhibitors are competitive at the ATP binding site, resulting in a lack of specificity among kinases.[9,11,12] Therefore, the task remains to inhibit CDK5 using a more effective approach. A longer-acting, safer, and more specific reduction of CDK5 is needed to control CDK5 overactivation in pathologic conditions.[13]

Viral vectors have become very common as effective RNA interference (RNAi) delivery systems to target regions to produce a sustained and controlled release of therapeutic molecules or to transport molecules across/infiltrate barriers. RNA interference silences of specific genes[14] and therefore may be used to reduce the expression of pathogenic genes, a promising approach for neurologic disorders.[15] Therefore, in this study, we evaluated the effect of CDK5 RNAi delivery in adeno-associated viral vectors

[1]Cellular and Molecular Neurobiology Area, Group of Neuroscience of Antioquia, School of Medicine, SIU, University of Antioquia UdeA, Medellín, Colombia and [2]Behavioral Neurophysiology Laboratory, School of Medicine, Universidad Nacional de Colombia, Bogotá, Colombia. Correspondence: Dr GP Cardona-Gómez, Sede de Investigación Universitaria (SIU), Universidad de Antioquia, Calle 62 # 52–59; Torre 1, Piso 4, Laboratorio 412, Medellín 05001000, Colombia.
E-mail: patricia.cardonag@udea.edu.co
The research reported in this publication was supported by Colciencias Projects #111551928905 and #111554531400 (GPC-G).
Received 15 December 2014; revised 25 May 2015; accepted 26 May 2015; published online 24 June 2015

(AAV) on the hippocampus, and its effect on cognitive and motor function after cerebral ischemia in rats.

MATERIALS AND METHODS

All of the animal procedures were performed in concordance with the ARRIVE guidelines, with the Guide for the Care and Use of Laboratory Animals, 8th edition, published by the National Institutes of Health (NIH) and according to Colombian standards (law 84/1989 and resolution 8430/1993). These procedures were approved by Ethics Committee for Animal Experimentation of the University of Antioquia, Medellín, Colombia.

Animal Model

Male Wistar albino rats from our in-house, pathogen-free colony at the vivarium at SIU (Sede de Investigación Universitaria), University of Antioquia, Medellin, Colombia, were kept on a 12:12-hour dark:light cycle and received food and water *ad libitum*. Special care was taken to minimize animal suffering and to reduce the number of animals used. Three-month-old rats weighing 250 to 310 g were used. Fifteen rats per experimental group were used for neurologic scoring and the evaluation of spatial learning and memory. In addition, 4 to 6 rats per experimental group were used for the histologic and biochemical assessments.

Middle Cerebral Artery Occlusion

The animals were anesthetized with an intraperitoneal mixture of ketamine (60 mg/kg; Holliday Scott S.A. Int. Neyer, Buenos Aires, Argentina), xylazine (5 mg/kg; Synthesis LTDA & CIA S.C.A, Bogotá, Colombia) and subcutaneous atropine (100 mg/kg; ERMA S.A, Bogotá, Colombia). The rats received a mixture of 2% to 4% isoflurane (Baxter, Deerfield, IL, USA) and 96% oxygen via an inhalation anesthesia machine. Body temperature was monitored with a rectal thermometer throughout the entire surgery, and the rats were maintained in a condition of mild hypothermia (34°C to 35°C). The right common carotid artery was exposed and dissected. The right external carotid artery and the right internal carotid artery were exposed, and the first artery branches were cauterized by electrocoagulation (AARON bipolar cautery, Albany, NY, USA). A 4-0 monofilament nylon suture (Corpaul, Bogotá, Colombia) was inserted into the internal carotid artery from the external carotid artery to occlude the right middle cerebral artery (MCA) at its origin. The nylon filament tips had been previously rounded by flaming and were coated with poly-L-lysine solution (0.1% w/v, in deionized water; Sigma, St Louis, MO, USA). The suture was removed for reperfusion after 60 minutes, and the wound was closed.[16] Sham-operated animals underwent identical procedures, except for the suture insertion.

Short Hairpin RNAmiR Delivery

The RNAi (short hairpin RNAmiR, shRNAmiR) sequences for silencing CDK5 (CDK5miR) and a control scrambled RNA sequence (SCRmiR), as well as the viral particle production and *in vitro* model silencing validation, were based on Piedrahita *et al*.[17] The AAV particles were obtained from the Davidson Laboratory (University of Iowa Viral Vector Core). The animals were injected with 2.5 μL of AAV2.5.shSCRmiR.GFP or AAV2.5.shCDK5miR.GFP into the right hippocampus (bregma coordinates: −2.56 antero-posterior, 0.8 lateral, and 4.1 depth). The injections were performed during the transient middle cerebral artery occlusion (tMCAO) 30 minutes after the filament was inserted (therapeutic intervention performed during the ischemic phase). Intrahippocampal injections were performed with a 10-μL Hamilton syringe at a rate of 0.2 μL/min, and 5 minutes elapsed after the infusion before withdrawal of the syringe.

Physiologic Parameter Recordings

During the surgical procedures, the body temperature was monitored continuously using a rectal probe. Monitoring of the mean arterial blood pressure by a Power Lab Data Acquisition System (ML870, AD Instruments, Sydney, Australia); pH and arterial blood gases ($n = 10$ to 12) by an Epoc Blood Analysis System (Epoc BGEM test card from Alere, Waltham, MA, USA) was performed via an indwelling cannula that was inserted into the left femoral artery. The parameters were measured 15 minutes before the filament was inserted, during tMCAO, and after 15 minutes of reperfusion.

Neurologic Evaluation

The animals were evaluated from 6 to 15 days after MCAO ($n = 15$) in each experimental group. Neurologic function was scored on an 18-point scale. The composite neuroscore comprises six different neurologic tests: (1) spontaneous activity, (2) symmetry in limb movement, (3) forepaw outstretching, (4) climbing, (5) body proprioception, and (6) response to vibrissae touch. Each test was scored with a maximum of three points based on a set of predetermined criteria described elsewhere.[18] The scores for each test were summed for a highest possible score of 18, indicating no neurologic deficits, and lowest score of 3, for animals with the most severe impairment. Neurologic scoring was performed each day and in the same order for all rats.

Inclined Plane Test

All of the rats ($n = 15$) were also assessed from 6 hours to 15 days after MCAO using the inclined plane test.[19] Briefly, the device consists of a hinged board raised and lowered to different angles. The objective is for the rat to maintain itself on the board for 30 seconds as the angle is gradually increased at 5° intervals. The assigned score is the maximum angle of the plane that the rat can maintain itself for 30 seconds without sliding.

Water Maze Test

One month after ischemia, the rats ($n = 15$ per each experimental group) were trained and evaluated in the Morris water maze.[20] The apparatus consists of a black plastic tank (1.8 m in diameter and 0.6 m in height) filled with water (22 ± 2°C) to a depth of 35 cm. The platform (12-cm diameter) is located 3 cm below the water's surface during the spatial learning session and 2 cm above the water's surface during the visible session. Extra-maze visual cues around the room remained in a fixed position throughout the experiment. The first phase involved two daily sessions of learning. Each session consisted of four successive trials, and each trial began with a pseudorandom placement of the rat into one of four randomly located starting positions. Before the initial trial, the animals were trained to stay on the platform for 30 seconds. If the rat did not find the platform after a maximum of 90 seconds, then it was gently guided to the platform. Eight learning sessions were conducted to examine the spatial learning performance. Two days after the end of the learning phase, the animals were tested for retention with a 60-second probe trial without the platform. During the probe trial, the latency to reach the exact platform location and the number of crossings over platform site were determined. One day after the probe trial, the platform was moved to the opposite quadrant, and the animals underwent a transfer test to assess their cognitive flexibility and ability to solve a new spatial problem. To control for any differences in visual-motor abilities or motivation between the experimental groups, the latencies to reach the platform were evaluated using a visible platform (four trials) at the end of the retention test. Behavior performance was recorded by an automated system (Viewpoint, Lyon, France). Finally, the animals were killed for histologic and biochemical evaluation.

Determining Infarct Volume

The rats were transcardially perfused with 300 mL of 0.9% normal saline under deep anesthesia (ketamine/xylazine mixture) 6 days after tMCAO reperfusion, and their brains were carefully removed, cooled in phosphate-buffered saline for 5 minutes, and sliced coronally every 2 mm using a rat brain matrix (Stoelting Co., Wood Dale, IL, USA). The slices were stained by 0.5% 2,3,5-triphenyltetrazoilum chloride (TTC; Sigma) and dissolved in physiologic buffer solution for 30 minutes at 37°C in the dark.[21]

The sections were washed twice with saline, fixed with 4% paraformaldehyde for 30 minutes at room temperature, and then registered for image analysis. Brain infarct size was measured in ImageJ software (version 1.0; US National Institutes of Health, Bethesda, MD, USA), and infarct areas were integrated for calculating infarct volume. The total volume of each hemisphere and infarction was determined by integrating areas in each slice. Infarct volume was calculated using the following formula: infarct volume = [left hemisphere volume − (right hemisphere volume − measured infarct volume)]/left hemisphere volume. Infarct volume in each rat was corrected to compensate for brain swelling in the ischemic hemisphere[22] by computing left and right hemisphere volume and applying the following formula: corrected infarct volume = left hemisphere

volume – (right hemisphere volume – measured infarct volume). The infarction volume was expressed in cubic millimeters and as a percentage.

Histology

Anesthetized animals ($n = 4$ to 6 for each experimental group) were perfused with 4% paraformaldehyde in 0.1 mol/L phosphate buffer, pH 7.4. The brains were removed and postfixed with 4% paraformaldehyde at 4°C for 48 hours, rinsed with saline buffer and sectioned at 50 μm with a vibrating-blade microtome (VT1000S, Leica Microsystems, Nussloch, Germany). Cerebral cortex was analyzed in the coronal section 2.6 mm anterior to bregma, the hippocampus were analyzed in coronal sections 2.56, 3.60, and 5.20 mm posterior to bregma.

The neuronal populations and morphology were evaluated in CA1 antero-posterior serial sections using Nissl staining with toluidine blue (Sigma). Briefly, the sections were rinsed in distilled water and then immersed in 1% toluidine blue; the slides were dehydrated, immersed in xylene, and mounted in Depex. The CA1 sections were photographed at $\times 10$ and $\times 40$ magnifications using a Nikon Eclipse E200 microscope (Kawasaki, Japan).

Immunohistochemistry

The sections were incubated while free-floating with moderate shaking. The sections were initially treated for 20 minutes at room temperature with methanol (50%, v/v) and hydrogen peroxide (1%, v/v) in 0.1 mol/L phosphate-buffered saline (PBS) at a pH of 7.4 to quench endogenous peroxidase. Then, the sections were incubated for 30 minutes at room temperature with Triton X-100 (0.5%, v/v) in 0.1 mol/L phosphate buffer. Nonspecific antibody binding sites were subsequently blocked by treating the sections for 30 minutes at room temperature with BSA (3%) and Triton X-100 (0.3%, v/v) in 0.1 mol/L PBS. The sections were incubated overnight at 4°C using anti-MAP2 (monoclonal mouse 1:1,000, Chemicon, Temecula, CA, USA), anti-PHF-Tau (AT-8, 1:500, Pierce, Rockford, IL, USA), anti-Bax (rabbit 1:500; Santa Cruz, CA, USA), and anti-pCREB (mouse 1:500, Cell Signaling Technology, Beverly, MA, USA) antibodies. After several rinses in PBS, the sections were incubated for 90 minutes at room temperature with biotinylated mouse or rabbit secondary antibodies (Pierce; diluted 1:250). The sections were washed four times in PBS and incubated for 1 hour with avidin/biotin peroxidase (1:250; Pierce). Peroxidase was revealed using diaminobenzidine. The sections were mounted on slides, dehydrated, washed with PBS, and covered with coverslips using Vecta-shield mounting medium (Vector Laboratories, Burlingame, CA, USA). Omission of the primary antibodies resulted in no staining. The sections were photographed at $\times 10$ and $\times 40$ magnifications using a Nikon Eclipse E200 microscope. Microphotographs were analyzed using ImageJ (version 1.0; US National Institutes of Health, Bethesda, MD, USA) to evaluate microtubule-associated protein 2 (MAP2), AT8, Bax, and pCREB immunoreactivity intensities in a total area of 1.2288 mm^2 (×10). The images were modified to a binary system and integrated densities (relative units), which were obtained for each image. The background was automatically subtracted in each image to quantify the relative intensity of immunostaining.

Immunofluorescence

The sections at the level of bregma were rinsed in 0.1 mol/L PBS and incubated for 10 minutes with 50 mmol/L ammonium chloride to avoid autofluorescence. Then, the sections were preincubated for 60 minutes at room temperature with Triton X-100 in PBS (TXPBS) and 3% BSA. The sections were incubated overnight at 4°C with the following primary antibodies: anti-GFAP (monoclonal mouse, 1:1,000; Chemicon, Temecula, CA, USA), anti-OX42 (polyclonal rabbit, 1:1,000; Millipore, Bedford, MA, USA), anti-NeuN (Monoclonal mouse, 1:1,000; Millipore) and anti-CDK5 (C-8) (1:1,000; Santa Cruz, CA, USA). The primary antibodies were diluted in TXPBS and 1% BSA. Then, the sections were washed four times in 0.1 mol/L PBS and incubated for 90 minutes at room temperature with mouse and rabbit Alexa Fluor 594 secondary antibody (1:2,000; Molecular Probes, Eugene, OR, USA). The sections were washed four times in buffer, mounted on slides and coverslipped using Gel Mount (Biomeda, Hatfield, PA, USA). The sections were observed and photographed with a motorized spinning disk confocal microscope (Disk Scan Unit) Olympus IX 81 (Olympus, Latin America, Inc., Miami, FL, USA). Omission of the primary antibodies resulted in no staining. The sections were photographed at $\times 10$, $\times 40$, and $\times 60$ magnifications. Those images were analyzed evaluating the fluorescence intensity (FI) of CDK5, GFAP, and OX42 immunostaining at $\times 10$ using Cell M (Olympus software, Miami, FL, USA).

Western blotting

Animals ($n = 4$ to 6 per each experimental group) were killed by decapitation, and their brains were quickly removed. The ipsilateral CA1 was dissected and frozen at − 80°C until analysis. The samples were homogenized in lysis buffer containing 150 mmol/L NaCl, 20 mmol/L Tris, pH 7.4, 10% glycerol, 1 mmol/L EDTA, 1% NP-40, 100 μmol/L phenylmethylsulfonyl fluoride, 1 μg/mL aprotinin and leupeptin (Sigma) and 100 μmol/L orthovanadate. The lysates were clarified by centrifugation at 15,366 gs for 5 minutes. Sodium dodecyl sulfate-polyacrylamide gel electrophoresis (SDS-PAGE; 10%) was performed using a mini-protean system (Bio-Rad) with low-range molecular-weight standards (Bio-Rad Laboratories, Hercules, CA, USA). Protein (30 μg) was loaded onto each lane with loading buffer containing 0.375 mol/L Tris, pH 6.8, 50% glycerol, 10% SDS, 0.5 mol/L DTT and 0.002% bromophenol blue. The samples were heated at 100°C for 3 minutes before gel loading. After electrophoresis, the proteins were transferred onto nitrocellulose membranes (Amersham, Buckinghamshire, UK) using an electrophoretic transfer system (mini Trans-blot Electrophoretic Transfer Cell) at 250 mA for 2 hours. The membranes were then washed with tris-tween buffered saline (20 mmol/L Tris-HCl, pH 7.5, 500 mmol/L NaCl, 0.05% Tween-20 containing Tris-buffered saline solution, pH 7.4) and 5% nonfat dry milk for 30 minutes. Tris-tween buffered saline was used for all successive washings and incubations. The membranes were first incubated overnight at 4°C with the following primary antibodies: rabbit anti-CDK5 (C-8) (1:1,000; Santa Cruz, CA, USA), rabbit anti-p35/p25 (1:500; Santa Cruz, CA, USA), rabbit cyclic AMP response element-binding protein (CREB) (1:1,000; Cell Signaling Technology), mouse pCREB (1:1,000; Cell Signaling Technology), rabbit Tropomyosin Receptor kinase B (TRKB) (1:1,000; Millipore); mouse extracellular signal-regulated kinase 1/2 (ERK1/2) (1:1,000; Cell Signaling Technology), mouse phospho ERK 1/2 (pERK1/2) (1:1,000; Millipore); mouse pCAMKII (1:1,000; Cell Signaling Technology), rabbit AKT (1:1,000; Millipore), and mouse pAKT (1:1,000; Millipore). The membranes were incubated with goat anti-rabbit IRDye 800WE secondary antibody (Li-COR, Lincoln, NE, USA), and staining was detected using the ODYSSEY Infrared Imaging System (Li-COR, Miami, FL, USA). The band intensities were measured with ImageJ Software (NIH) and normalized to the intensities of control tubulin values (1:2,000 Promega). The results for each membrane were normalized to control values. The samples from all of the experimental groups were processed in parallel to minimize interassay variation.

Cyclin-Dependent Kinase 5 Assay

CA1 was dissected and rapidly frozen in liquid nitrogen. The brain tissues were kept at − 70°C to preserve enzymatic activity until the assay was performed. The samples were homogenized in lysis buffer containing 150 mmol/L NaCl, 20 mmol/L Tris, pH 7.4, 10% glycerol, 1 mmol/L EDTA, 1% NP-40, 100 μmol/L phenylmethylsulfonyl fluoride, 1 μg/mL aprotinin and leupeptin (Sigma), and 100 μmol/L orthovanadate. The lysates were clarified by centrifugation at 15366 gs for 5 minutes. Cyclin-dependent kinase 5 was immunoprecipitated from 250 μg of total protein using 1 μg of IgG rabbit polyclonal anti-CDK5 (C-8) antibody (Santa Cruz, CA, USA). The antibody and the protein extract were incubated overnight at 4°C in a rotator. After the addition of protein G sepharose (Sigma), the sample was incubated for an additional 1 hour at 23°C. Then, the protein G sepharose beads were washed five times with IP buffer (Sigma), keeping the sample at 4°C. After the fifth wash, the protein G sepharose beads were resuspended in 200 μL of kinase assay buffer (20 mmol/L Tris/HCl, pH 7.5, 100 μmol/L sodium orthovanadate, 10 mmol/L $MgCl_2$, 50 mmol/L NaCl, 1 mmol/L DTT, and 1 mmol/L NaF), and a 10-fold excess of ATP (0.5 mmol/L) was added to the resuspended beads. Histone from calf thymus type III-S (Sigma) was added as a substrate for CDK5 at a final concentration of 6 μmol/L, and the reaction mixture was gently vortexed and incubated at 37°C for 30 minutes. To stop the reaction, 5 μL of SDS-PAGE loading buffer (250 mmol/L Tris-HCl, 10% SDS, 30% glycerol, 0.5 mol/L DTT, and 0.02% bromophenol blue) was added, immediately followed by a 5-minute incubation at 95°C. The samples were separated electrophoretically at 120 V/2 hours and transferred onto a nitrocellulose membrane at 200 mA/1.5 hours. The histone band was clearly visible, and its migration on the gel was identified at approximately 21 kDa. Western blotting detection using anti-CDK5 (C-8 antibody) and rabbit polyclonal anti-histone H1 phosphorylated (Millipore) was performed. Goat anti-rabbit

IRDye 800WE (Li-COR) was used and detected using ODYSSEY Infrared Imaging System (Li-COR). The band intensities for histones were measured with ImageJ Software (NIH) and relativized to the total amount of initial CDK5, which was relativized to the loading control (tubulin).

Calpain Activation Assay

The ipsilateral hippocampi were homogenized in 20 mmol/L Tris-HCl, 137 mmol/L NaCl, 1% NP-40, 10% glycerol, 1 mmol/L phenylmethylsulfonylfluroide, 10 μg/mL aprotinin, 1 μg/mL leupeptin, and 0.5 mmol/L sodium vanadate. The homogenates were centrifuged at 14,000 *g* for 5 minutes, and the supernatants were collected for Calpain immunoassay. Calpain activity was measured using a commercially available kit (Calpain-Glo protease assay, Promega), according to the manufacturer's instructions. The samples were assayed by duplicate. Human calpain-1 (Tocris-Bioscience, Bristol, UK) was used as a positive control, and the calpain activity from hippocampal lysates was measured using a luciferase-based assay on a microplate luminometer (GlioMax, Promega).

Brain-Derived Neurotrophic Factor Immunoassay

The ipsilateral hippocampi were homogenized in 20 mmol/L Tris-HCl, 137 mmol/L NaCl, 1% NP-40, 10% glycerol, 1 mmol/L phenylmethylsulfonylfluroide, 10 μg/mL aprotinin, 1 μg/mL leupeptin, and 0.5 mmol/L sodium vanadate. The homogenates were centrifuged at 14,000 *g* for 5 minutes, and the supernatants were collected for brain-derived neurotrophic factor (BDNF) immunoassay. All of the samples were subjected to BDNF quantification by a commercially available kit (BDNF Emax Immunoassay system; Promega), according to the manufacturer's instructions. The samples were assayed in duplicate using 96-well plates that were subjected to overnight coating with anti-BDNF monoclonal antibody. A BDNF standard dilution series was also applied to obtain the absorbance–concentration calibration curve. The concentration values were normalized to the total protein concentrations of the corresponding lysates.

Sample Size, Randomization, Statistical Analysis

Animals were randomly allocated upon arrival from the breeding colony to sham or ischemia groups. After the surgery, we again randomly assigned those animals treated with SRCmiR or CDK5miR. The sample size was determined based on the previous ischemia studies in our laboratory,[16,23,24] which showed that the effects of ischemia are reproducible with a minimal number of animals.

Four to six rats per experimental group were histologically and biochemically analyzed, 15 animals per group were studied for behavioral experiments (neurologic scores and water maze test), and 10 to 12 animals per group were analyzed for physiologic parameter measurements. In this study, there was a 12.76% mortality due to the cerebral ischemia procedure. The animals that did not learn the water maze tasks or did not present AAV GFP (green fluorescent protein) expression in the hippocampus by histologic analyses were excluded from the study. The sample sizes (*n*) used for statistical analyses were the number of animals per experimental group. The homogeneity of variance test was applied before statistical analysis. The parametric data were compared using one-way analysis of variance (ANOVA) with Tukey's *post hoc* test for comparing several independent groups in the physiologic, histologic, and biochemical analyses. The behavioral experiment results, neurologic scores, inclined plane test performances, and escape latencies during the training and transfer tests (water maze) were examined by repeated measures ANOVA, also ANOVA per day followed by Fisher's *post hoc* test were realized. The probe trial (water maze) results were analyzed by ANOVA followed by Fisher's *post hoc* tests. The analyses were performed with SPSS 18.0 (Chicago, IL, USA). The data are expressed as the mean ± the s.e.m., $P < 0.05$. To diminish interassay variation, all of the sample groups were processed in parallel.

RESULTS

Physiologic Parameters Before, During, and After Cerebral Ischemia

The physiologic parameters obtained before, during, and after focal cerebral ischemia and stereotaxic injection from sham and ischemic animals are shown in Table 1. The baseline data are presented in the sham SCRmiR group. Before injection with CDK5miR or SCRmiR, no significant differences were observed among the sham and ischemic groups.

Under the basal condition, the arterial blood pressure was 76.7 ± 6.63 mm Hg Arterial pressure increased in both the SRCmiR and CDK5miR ischemic groups during the arrest of carotid blood flow to 89.7 ± 3.34 and 89.4 ± 2.27 mm Hg, respectively ($P = 0.047$). Additionally, the pH increased to 7.4 ± 0.01 in both of the ischemic groups compared with 7.3 ± 0.02 in both of the sham groups ($P = 0.026$). Moreover, pCO_2 pressure was reduced to 42.8 ± 1.94 and 38.9 ± 1.94 mm Hg in the ischemic SRCmiR- and CDK5miR-treated rats, respectively, during the arrest of carotid blood flow. These results are compared with the control values of 55.1 ± 3.19 and 51.5 ± 2.63 in the SRCmiR and CDK5miR sham groups, respectively ($P = 0.042$). In the 15-minute recovery period after ischemia, no significant differences were observed between the sham and ischemic groups.

No significant differences in these physiologic variables were observed when we compared the two sham and two ischemic groups at different times before, during, and after ischemia.

CDK5miR Prevents Cyclin-Dependent Kinase 5 and Calpain Activities Upregulation at 1 Month After Ischemia Treatment

AAV2.GFP was widely expressed in the injected CA1 area (Figure 1Aa, b) in all of the experimental groups. We found a very weak GFP expression in the contralateral hemisphere (Figure 1A). CDK5miR produced a significant reduction in CDK5 FI in the sham rats (20%, $P < 0.05$; Figure 1Aa, c). Is contrast, the ischemic animals treated with SRCmiR exhibited a notable increase in CDK5 immunoreactivity (60%, $P < 0.001$), which was reduced by the CDK5miR treatment (70%, $P < 0.001$) (Figure 1Aa, c). The data showed that CDK5 activity was also reduced by 20% ($P < 0.05$) and 40% ($P < 0.001$) in the sham and ischemic animals treated with CDK5miR (Figure 1B). Those results were accompanied by an observed increase in p25 protein levels in the ischemic hippocampus (50%, $P < 0.05$) compared with the control values and a significant reduction (60%) due to CDK5miR treatment ($P < 0.05$) (Figure 1C). However, the total p35 protein levels, p25/p35 ratio, and total CDK5 levels remained unchanged (Figure 1Cb–d). Interestingly, we observed higher calpain activation in ischemic animals treated with SRCmiR compared with the sham groups, and this effect was significantly reduced by the CDK5miR treatment (Figure 1D).

Cyclin-Dependent Kinase 5 Downregulation Reduces Infarct Volume and Accelerates Motor Function Recovery in the First Week After Ischemia

Motor impairment was evaluated from 6 hours to 15 days after ischemia. Ischemic animals exhibited significantly lower neurologic scores than the sham-operated animals during the first 15 days after surgery ($P < 0.001$). During days 5 to 7 after ischemia, the CDK5miR-treated animals displayed neurologic scores that were significantly higher than the SCRmiR-treated animals ($P < 0.05$; Figure 2A). Neither CDK5miR nor SCRmiR treatment produced significant changes in the sham-operated subjects' performance in the inclined plane test. In contrast, ischemic animals maintained themselves at significantly lower angles, confirming ischemia-induced motor impairment. The CDK5 interference in the ischemic animals produced a significant improvement during days 4 to 7 after tMCAO compared with the SCRmiR treatment (Figure 2B). The CDK5 knockdown itself did not affect neurologic or motor performance in the sham rats.

Therefore, considering the neurologic and motor recovery data, the beneficial effects of CDK5 silencing were concluded to take place between 5 and 7 days after injection. Choosing an intermediate time point, we assessed infarct volume and expression of CDK5 in motor cortex and CA1 region at 6 days after ischemia. SCRmiR-treated ischemic rats presented a remarkable infarct

Table 1. Physiologic measurements before, during, and after ischemia and stereotactic injection

	Sham-shSRCmiR	*Sham-shCDK5miR*	*Ischemia-SRCmiR*	*Ischemia-CDK5miR*	
Before surgery (15 minutes)					
Arterial blood pressure(mm Hg)	66.8 ± 2.64	64.3 ± 1.37	69.2 ± 3.09	71.7 ± 1.14	n.s.
pH	7.3 ± 0.01	7.3 ± 0.02	7.3 ± 0.04	7.3 ± 0.04	n.s.
pCO_2 (mm Hg)	55.6 ± 2.42	53.2 ± 1.79	53.1 ± 5.75	49.3 ± 5.75	n.s.
pO_2 (mm Hg)	267.1 ± 32.85	261.8 ± 32.15	225.2 ± 38.88	220.1 ± 38.88	n.s.
Glucose (mg/dL)	306.8 ± 19.46	332.2 ± 34.69	305.2 ± 29.10	295.5 ± 8.47	n.s.
Lactate (mmol/L)	0.7 ± 0.17	0.9 ± 0.12	0.9 ± 0.11	0.9 ± 0.36	n.s.
Hematocrit	39 ± 2.073	41 ± 0.71	39.7 ± 0.86	41.7 ± 1.03	n.s.
Sodium (mmol/L)	148.6 ± 4.89	146 ± 2.43	144.75 ± 0.25	147.5 ± 3.84	n.s.
Potasium (mmol/L)	4.3 ± 0.31	4.6 ± 0.14	4.2 ± 0.01	4.2 ± 0.11	n.s.
Calcium (mmol/L)	1.3 ± 0.09	1.3 ± 0.03	1.4 ± 0.02	1.3 ± 0.06	n.s.
Temperature (°C)	34.2 ± 0.12	34.5 ± 0.38	34.15 ± 0.56	33.875 ± 0.43	n.s.
During surgery (15 minutes)					
Arterial blood pressure (mm Hg)	76.7 ± 6.63	74.7 ± 1.42	89.7 ± 3.34*	89.4 ± 2.27*	$P = 0.04$
pH	7.3 ± 0.02	7.3 ± 0.018	7.4 ± 0.01*	7.4 ± 0.01*	$P = 0.026$
pCO_2 (mm Hg)	55.1 ± 3.19	51.5 ± 2.63	42.8 ± 1.94*	38.9 ± 1.94*	$P = 0.042$
pO_2 (mm Hg)	268.8 ± 36.29	271.5 ± 37.68	236.9 ± 33.21	230.6 ± 33.21	n.s.
Glucose (mg/dL)	310.2 ± 28.65	321.4 ± 28.91	325.2 ± 34.66	296 ± 19.01	n.s.
Lactate (mmol/L)	1.034 ± 0.19	0.85 ± 0.20	0.93 ± 0.17	1.04 ± 0.08	n.s.
Hematocrit	42.2 ± 0.73	42.2 ± 1.28	41.5 ± 1.66	42.5 ± 1.55	n.s.
Sodium (mmol/L)	142.2 ± 0.49	142.2 ± 1.32	142.5 ± 0.29	143.5 ± 2.10	n.s.
Potasium (mmol/L)	4.76 ± 0.19	4.58 ± 0.14	4.35 ± 0.13	4.37 ± 0.15	n.s.
Calcium (mmol/L)	1.4 ± 0.04	1.4 ± 0.04	1.3 ± 002	1.3 ± 0.06	n.s.
Temperature (°C)	34.14 ± 0.58	34.46 ± 0.10	33.9 ± 0.49	33.7 ± 0.32	n.s.
After surgery (15 minutes)					
Arterial blood pressure (mm Hg)	80.6 ± 8.73	80.3 ± 6.60	86.3 ± 1.78	89.7 ± 5.178	n.s.
pH	7.3 ± 0.03	7.3 ± 0.02	7.3 ± 0.01	7.3 ± 0.01	n.s.
pCO_2 (mm Hg)	52.1 ± 5.68	51.9 ± 3.1577	45.1 ± 1.77	45.4 ± 1.77	n.s.
pO_2 (mm Hg)	273.7 ± 19.86	254 ± 28.15	242.1 ± 24.05	268.6 ± 24.05	n.s.
Glucose (mg/dL)	306.8 ± 20.35	290.2 ± 29.27	305 ± 26.51	283.8 ± 9.49	n.s.
Lactate (mmol/L)	0.8 ± 0.20	0.9 ± 0.27	1 ± 0.15	1 ± 0.13	n.s.
Hematocrit	41.6 ± 0.75	42.2 ± 0.8	41.2 ± 2.35	41.7 ± 0.63	n.s.
Sodium (mmol/L)	142.6 ± 0.68	143 ± 1.26	141.7 ± 0.75	142.5 ± 1.32	n.s.
Potasium (mmol/L)	4.7 ± 0.23	4.8 ± 0.12	4.5 ± 0.17	4.5 ± 0.11	n.s.
Calcium (mmol/L)	1.4 ± 0.019	1.4 ± 0.03	1.3 ± 0.06	1.3 ± 0.05	n.s.
Temperature (°C)	33.46 ± 0.273	34.22 ± 0.239	33.45 ± 0.67	33.25 ± 0.466	n.s.

Values are mean ± s.e.m., SHAM: Simulation (Control), ISCHEMIA: t-MCAO, transient middle cerebral artery occlusion. The data are expressed as the group mean ± s.e.m. *Significant differences: *$P < 0.05$; $n = 10$ to 12 animals/group.

volume ($55.2 \pm 7.2\ mm^3$), and this effect was significantly reduced by the CDK5miR treatment ($18 \pm 3.2\ mm^3$) (Figure 2Ca, b). These results suggest a high neuroprotective capacity of CDK5miR at 6 days after ischemia in cerebral areas that were not directly transduced. We then determined the CDK5 FI, finding that ischemic animals treated with SRCmiR exhibited increased CDK5 immunoreactivity. This effect was also reduced in the motor cortex (Figure 2Da, b; $P < 0.001$) and in the CA1 hippocampal region (Figure 2Da, c; $P < 0.005$) by the CDK5miR treatment. We did not observe GFP expression in the motor cortex; expression was only observed in the CA1 injection site (Figure 2Da).

Cyclin-Dependent Kinase 5 Downregulation Prevents Cognitive Impairment at 1 Month After Ischemia

The effect of CDK5 interference on ischemia-induced impairments of hippocampus-dependent spatial tasks was examined using the Morris water maze. SCRmiR-treated ischemic animals spent more time ($P < 0.001$; Figure 3Aa) and traveled longer distances ($P < 0.001$; Figure 3Ab, c) to find the hidden platform than the sham-operated animals. In contrast, CDK5miR-treated ischemic animals exhibited better performances than the SCRmiR-treated ischemic animals ($P < 0.001$) (Figure 3Aa, b).

Forty-eight hours after the last training trial, the platform was removed from the maze. The SCRmiR-treated ischemic rats performed more poorly than the sham-operated groups, requiring a longer latency to reach the original platform position and lower number of crossings over the platform site. In contrast, the performance of the ischemic animals treated with CDK5miR did not differ from the sham-operated animals ($P < 0.05$; Figure 3Ba, b).

Three additional training trials were conducted with the hidden platform located on the opposite quadrant with respect to the original location. These tests were performed to evaluate the animals' reversal learning abilities. In contrast to the CDK5miR-treated ischemic animals, the SCRmiR-treated ischemic rats displayed impaired performance in reversal learning compared with the sham-operated rats, taking a longer time to find the new platform location ($P < 0.001$; Figure 3Ca). Furthermore, reversal learning impairment was revealed by analyzing the number of crossings over each quadrant during each reversal learning trial (Figure 3Cb, c). Therefore, we found that the SCRmiR ischemic animals exhibited fewer crossings in quadrant A in the third trial ($P < 0.05$; Figure 3Cc). These findings indicate that SCRmiR-treated ischemic rats not only forgot the original platform position (quadrant A) but also had an impaired ability to find the platform in a new location (quadrant C), presenting more crossings over quadrants B and D (different from those containing platform targets). In contrast, the CDK5miR-treated ischemic

animals persistently crossed quadrant A and quadrant C during the third trial (Figure 3Cc; $P < 0.05$), suggesting that these animals did not forget the original platform position and were also able to learn the new location. No significant differences among the groups were observed in the visible platform test (data not shown).

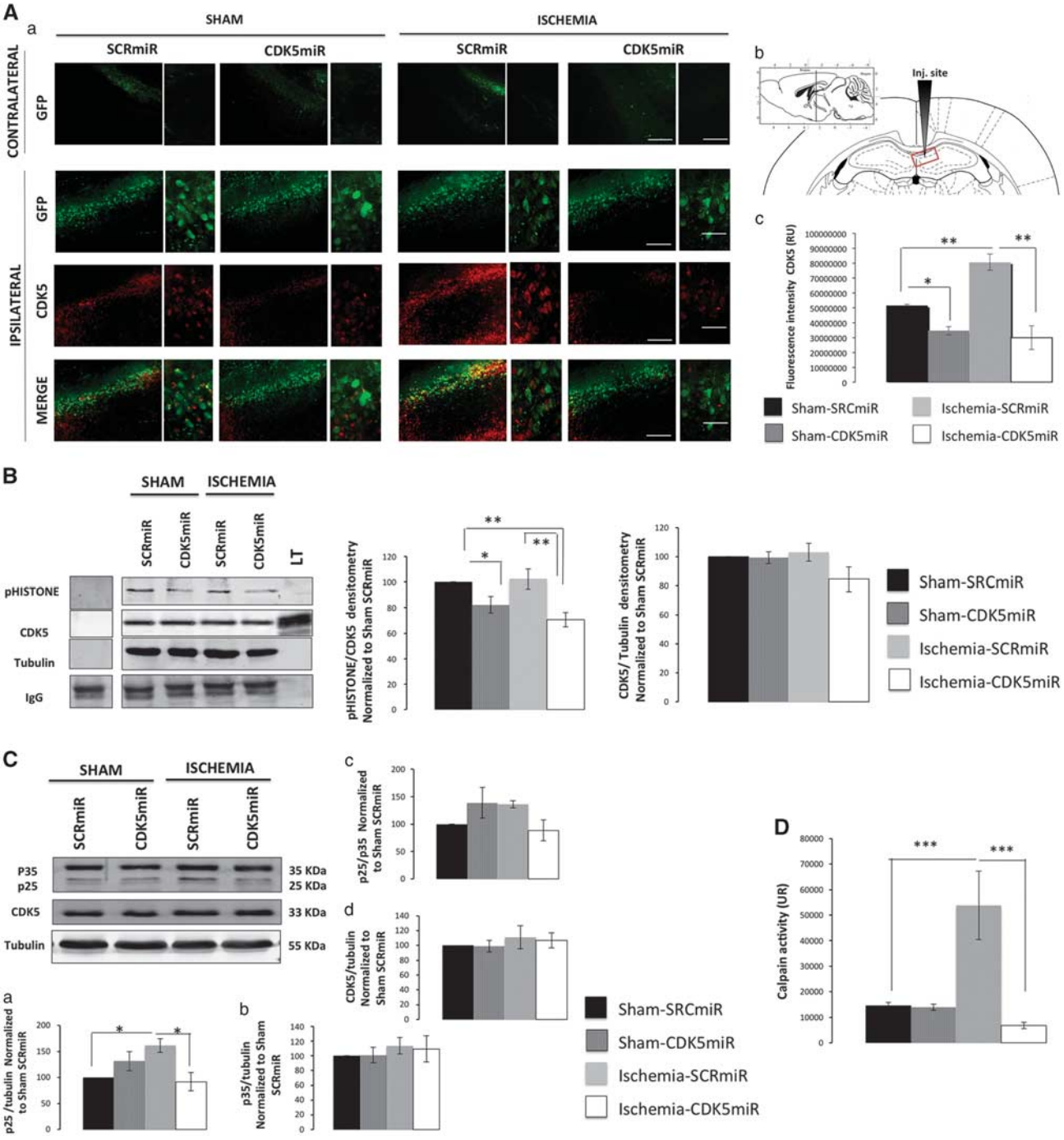

Figure 1. CDK5miR prevents CDK5 and calpain activities in ischemic rats at 1 month after ischemia. (**A**) CDK5 expression in CA1 (bregma − 2.56). (a) Green fluorescent protein (GFP) represents the transduced CA1 cells in the contralateral and ipsilateral hemispheres. (b) The sections were photographed at × 10 and × 40, scale bars = 50 μm (×10) and 25 μm (×40). The animals were killed 1 month after CDK5miR or SCRmiR were unilaterally injected into the right CA1 region. (c) Quantification of the fluorescence intensity of CDK5 immunoreactivity of transduced neurons using the software image Scope-Pro from Media Cybernetics. $n = 4$ to 6, $^{*}P < 0.05$; $^{**}P < 0.001$. (**B**) The ipsilateral CA1 was dissected, and CDK5 kinase activity was detected using a phosphorylated histone antibody. A band corresponding to the IgG heavy chain was detected. Densitometric quantification was performed. pHISTONE was relativized respect to the total CDK5 from lysates, relativized to the loading control (tubulin). $n = 4$ to 6, $^{**}P < 0.001$. (**C**) (a) CDK5, (b) p35, and (d) CDK5 protein levels from the CA1 regions of animals treated with SCRmiR and CDK5miR. Representative bands from western blotting are shown. (c) The p25/p35 ratio was established. Densitometric quantification was relativized to the loading control (tubulin) and normalized to the internal control (SCRmiR-treated sham rats). The values are mean ± s.e.m. (**D**) Calpain activity was measured in the ipsilateral CA1 region. $n = 4$ to 6, $^{*}P < 0.05$, $^{***}P < 0.0001$. CDK5, cyclin-dependent kinase 5; RU, relative units; SCR, scrambled RNA sequence.

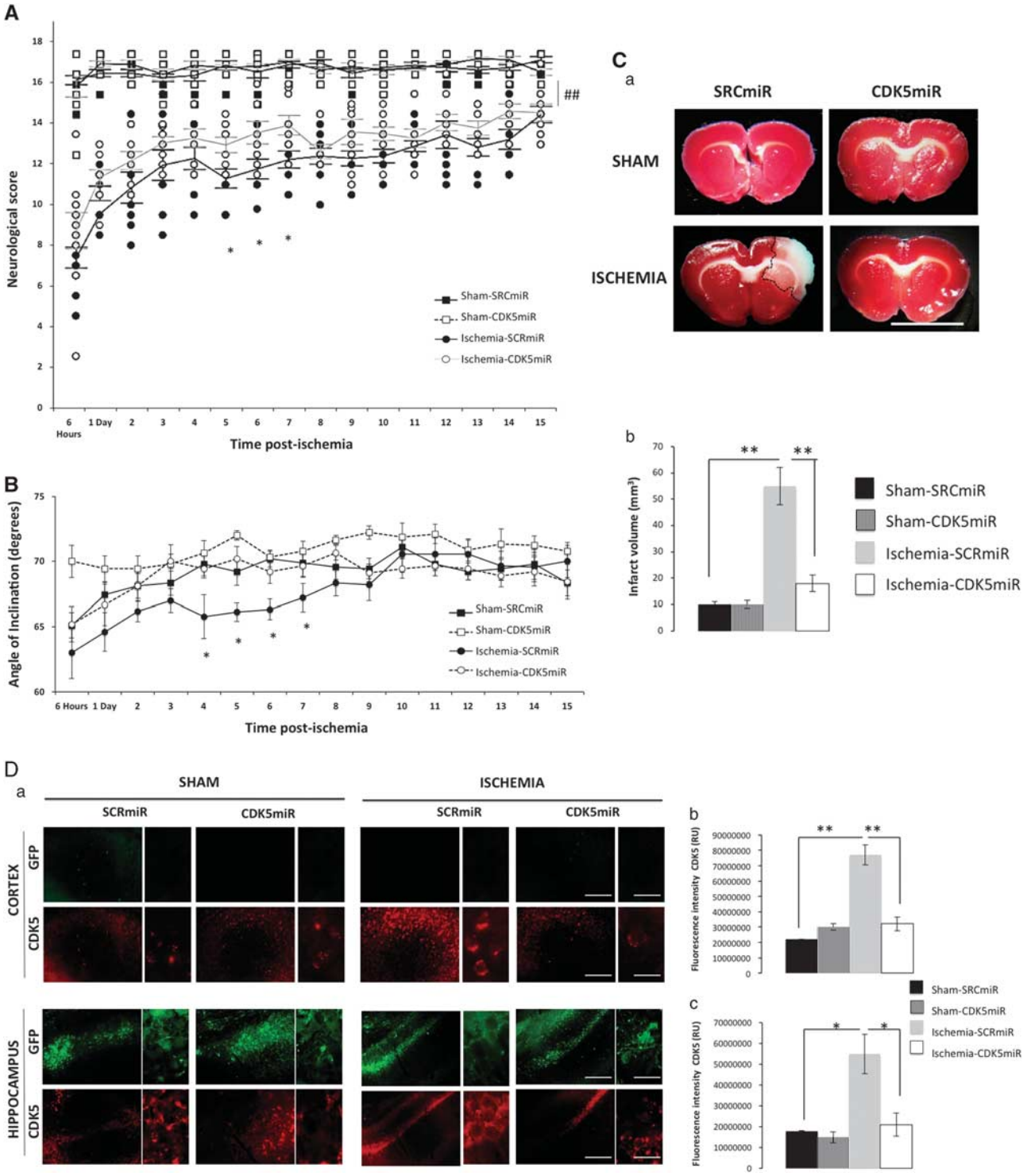

Figure 2. The protective actions of CDK5miR on neurologic function 1 week after ischemia. (**A**) Neurologic score during the 15 days after ischemia. $^{*}P < 0.05$, $^{\#\#}P < 0.001$. (**B**) The inclined plane test was scored from 6 hours to 15 days after ischemia. $^{*}P < 0.05$; $n = 15$ animals/group. (**C**) (a) Representative 2,3,5-triphenyltetrazoilum chloride (TTC) staining at 6 days after ischemia from animals treated with SCRmiR and CDK5miR (coronal sections at bregma 2.56). (b) The infarct volume quantification in cubic millimeters. (**D**) CDK5 expression in motor cortex and the CA1 anterior section. (a) Representative images of green fluorescent protein (GFP) and CDK5 fluorescences in the motor cortex (bregma 2.56) and CA1 (bregma −2.56) regions of the ipsilateral hemisphere. The sections were photographed at ×10 and ×40, scale bars = 50 μm (×10) and 15 μm (×60). (b) Fluorescence intensity of CDK5 immunoreactivity in the motor cortex and (c) in CA1 using the software image Scope-Pro Media Cybernetics. The data are expressed as the mean ± s.e.m. $n = 4$ to 6, $^{*}P < 0.05$; $^{**}P < 0.001$. CDK5, cyclin-dependent kinase 5; RU, relative unit; SCR, scrambled RNA sequence.

Silencing of Cyclin-Dependent Kinase 5 Prevents Hippocampal Neurodegeneration After Ischemia

Ischemic injury induces neural damage in the hippocampal CA1 field at 1 month after ischemia (Figure 4). Morphologic changes in the CA1 pyramidal cells were assessed by Nissl staining. The results showed that hippocampal cells in the sham animals had round and pale stained nuclei, which is typical of normal healthy cells (Figure 4A). Ischemic animals treated with SCRmiR exhibited neuronal shrinkage (Figure 4A), whereas the silencing of CDK5 attenuated the ischemic-induced alterations in the cells

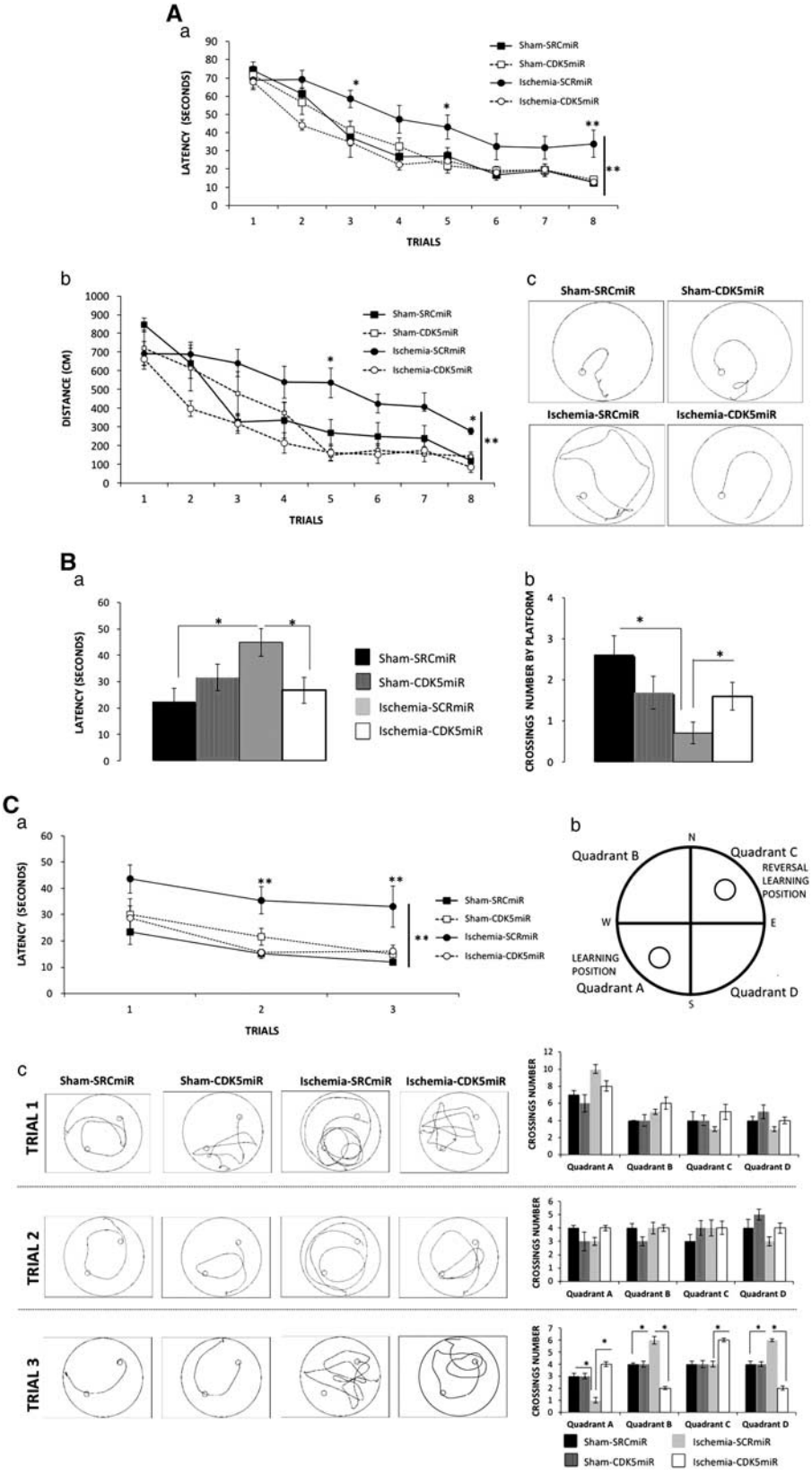

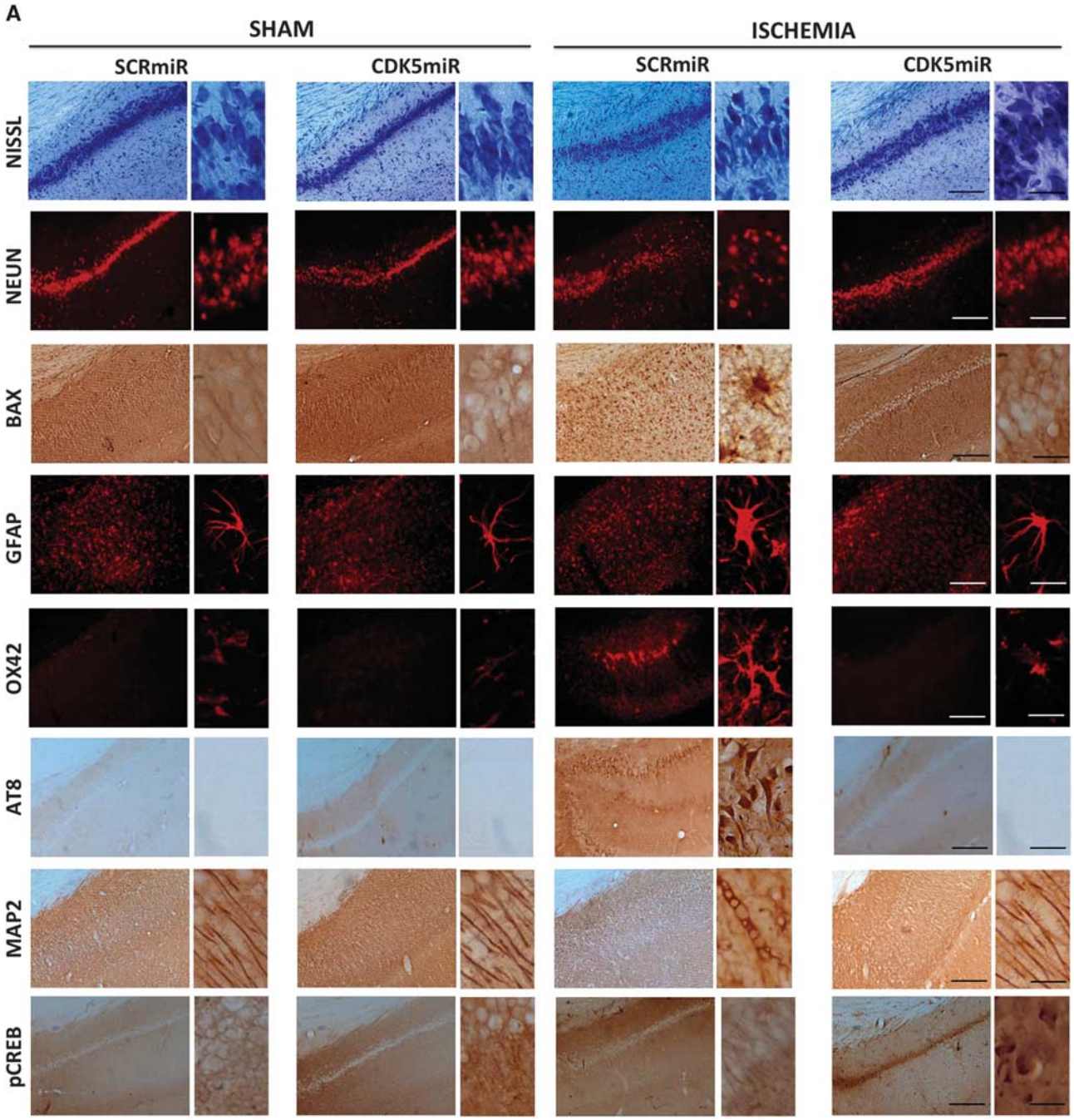

Figure 4. Cyclin-dependent kinase 5 (CDK5) silencing reduces neurodegenerative hallmarks in CA1 area at 1 month after ischemia. (**A**) Representative immunoreactivity levels from the ipsilateral CA1 region of the hippocampus (bregma − 2.56) at 1 month after ischemia are shown. The micrographs were obtained at × 10 and × 40. Scale bars: 50 μm (×10) and 25 μm (×40). (**B**) Immunoreactivity or fluorescence intensities of (a) NeuN, (b) BAX, (c) GFAP, (d) OX42, (e) AT8, (f) microtubule-associated protein 2 (MAP2), and (g) pCREB. These values were quantified at bregma levels of − 2.56, − 3.60, and − 5.20. *Significant differences, $P \leqslant 0.05$; $n = 4$ to 6 animals/group. CREB, cyclic AMP response element-binding protein; RU, relative unit; SCR, scrambled RNA sequence.

Figure 3. CDK5miR prevents learning and memory deficits 1 month after ischemia. Spatial learning and memory function were assessed with the Morris water maze test. (**A**) (a) Learning: average latency to find the hidden platform, (b) distance traveled to reach the platform, and (c) representative routes used to find the hidden platform in the final trial. (**B**) During the probe trial, (a) the latency to reach the exact platform location and (b) the number of crossings over the platform site was determined. (**C**) (a) Latency to reach the platform during reversal learning was established. (b) Quadrants of platform location were established as follows: quadrant A (position in learning) and quadrant B (position in reversal learning), with quadrants C and D outside the platform positions. (c) A representative route patterns traveled during the reversal learning test is shown, and the number of crossings in each quadrant during each trial in the reversal learning period were established. The data are expressed as the group mean ± s.e.m. *, **Significant differences: *$P < 0.05$, **$P < 0.001$; $n =$ 12 to 15 animals/group. CDK5, cyclin-dependent kinase 5; SCR, scrambled RNA sequence.

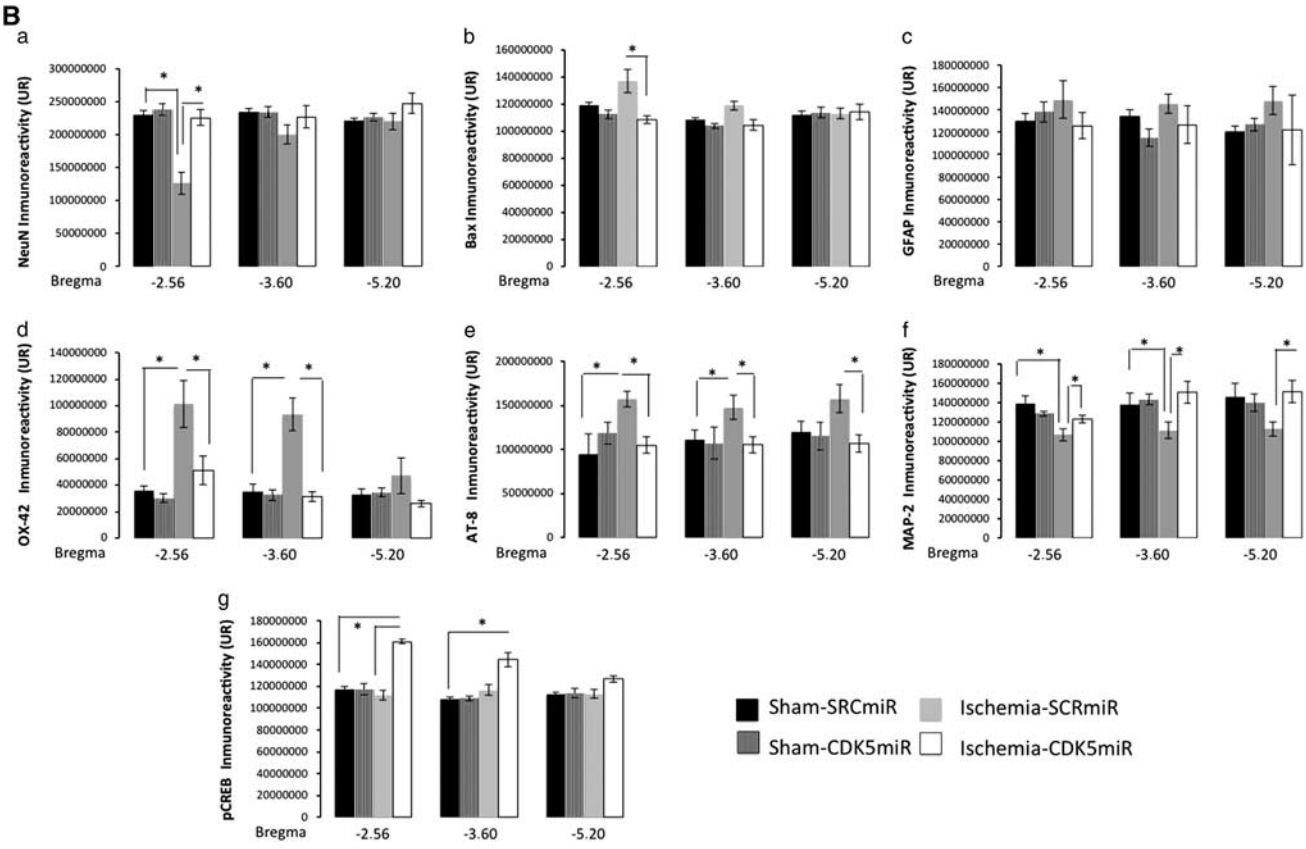

Figure 4. Continued.

(Figure 4A). This result was supported by NeuN and Bax immunoreactivity levels (Figures 4A and 4Ba, b), which showed a loss of neuronal nuclei and an increase in Bax expression in ischemic animals treated with SCRmiR. In contrast, animals treated with CDK5miR exhibited levels of NeuN FI and Bax immunoreactivity that were equivalent to those of sham control animals ($P < 0.05$; Figures 4A and 4Ba, b).

These results were supported by analysis of the astrocytic response, which constitutes one of the most prominent changes in the central nervous system after ischemic injury. The data showed that there were no significant differences among the groups in terms of the FI of GFAP immunoreactivity in the CA1 area (Figure 4Bc). Swollen and hypertrophic somas were observed in the astrocytes in response to ischemia, but the silencing of CDK5 reduced these changes (Figure 4A). We also found that the ischemic animals treated with SCRmiR presented a notable increase in microglial hyperreactivity (Figure 4A) at bregma levels of -2.56 ($P < 0.05$) and -3.60 ($P < 0.05$; Figure 4Bd). These observations confirm an infiltration of small and strongly Nissl-positive cells, indicating the presence of a substantial inflammatory response. The silencing of CDK5 resulted in the reduction of the inflammatory response by the OX42-IR indicator. This marker was less intense in CDK5miR-treated animals compared with the SCRmiR-treated ischemic animals ($P < 0.05$; Figures 4A and 4Bd) and was similar to the sham groups. The CDK5miR treatment itself did not produce hippocampal tissue alterations.

Hyperphosphorylated tau detected with AT8 (a phospho-specific PHF-tau antibody) was examined as a cognitive disorder-associated neurodegeneration marker. AT8-IR was absent in the sham groups, but extensive immunoreactivity was found in the ischemic animals treated with SCRmiR (Figure 4A) from bregma -2.56 ($P < 0.05$) to bregma -5.20 ($P < 0.05$; Figure 4Be). When we analyzed ischemic animals treated with CDK5miR, the tau pathology appeared to be reduced as assessed by immunodetection ($P < 0.05$; Figures 4A and 4Be). Additionally, we used an antibody against MAP2 to visualize the dendrites in the hippocampal formation. Consistently, MAP2 immunoreactivity (IR) in the CA1 region was diminished in ischemic animals treated with SCRmiR compared with the sham animals (Figure 4A) at bregma levels of -2.56 ($P < 0.05$), -3.60 ($P < 0.05$), and -5.20 ($P < 0.05$) (Figure 4Bf). The ischemic animals treated with CDK5miR exhibited a significant recovering of MAP2-IR, similar to the control values of the sham animals ($P < 0.05$; Figures 4A and 4Bf). Additionally, a hallmark of cerebral plasticity, pCREB, was detected. It is known that the transcription factor CREB has a key role in synaptic remodeling.[25] The CREB activation (phosphorylate CREB on serine 133, p-Ser133 CREB) leads to expression of genes encoding neuroprotective molecules, such as the anti-apoptotic protein Bcl-2, and contributes to the survival of neurons after ischemic insult. When we assessed the immunoreactivity of p-Ser133 CREB on the tissue, we found that pSer133-CREB-IR was weak in the sham and ischemic groups; however, extensive immunoreactivity was observed in the CDK5miR-treated ischemic animals ($P < 0.05$; Figure 4Bg).

Cyclin-Dependent Kinase 5 Silencing Promotes Plasticity Through Brain-Derived Neurotrophic Factor/Tropomyosin Receptor Kinase B Pathway After Cerebral Ischemia

We next evaluated the levels of BDNF, which is primarily synthesized by neurons in the adult brain and has a crucial role in plasticity.[26] Our data showed that ischemic animals SRCmiR had reduced levels of BDNF in the hippocampus as determined by ELISA ($P < 0.001$; Figure 5A). In contrast, CDK5miR-treated

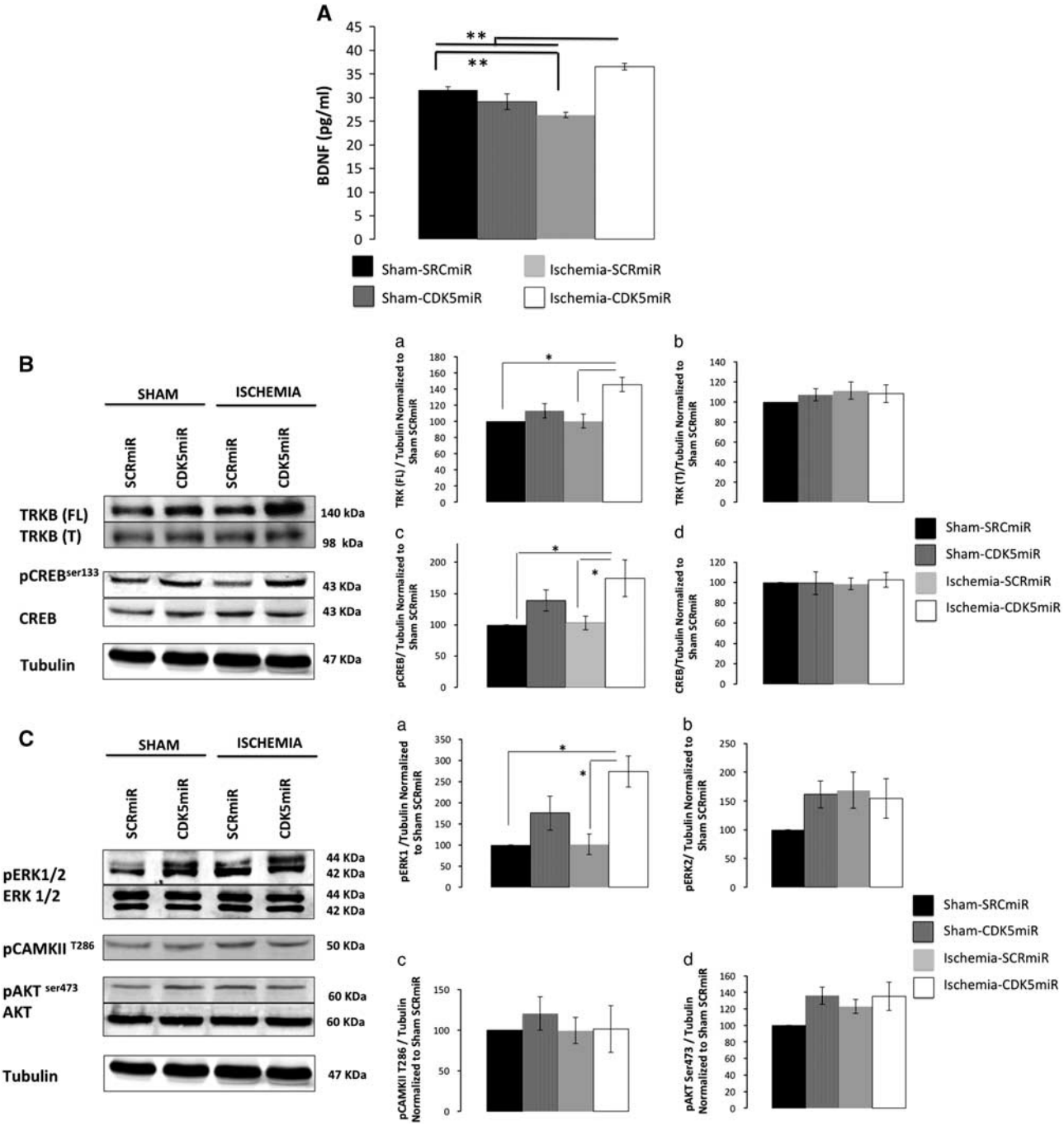

Figure 5. Cyclin-dependent kinase 5 (CDK5) silencing activated the BDNF/TRKB pathway 1 month after ischemia. (**A**) BDNF protein levels were measured in the hippocampus 1 month after ischemia. (**B**) Representative blots and total protein levels of (a) TrkB full length, (b) TrkB truncated, (c) pCREB (ser133), and (d) total CREB were determined by western blotting at 1 month after ischemia. (**C**) Representative blots and total protein levels of (a) pERK1, (b) pERK2, (c) pCAMKII Thr286, and (d) pAKt Ser473, which are involved in plasticity and survival. The protein levels were determined by western blotting at 1 month after ischemia. Densitometric quantification was relativized to the loading control (tubulin) and normalized to the internal control (SCRmiR-treated sham rats). The values are mean ± s.e.m. $n = 4$ to 6, $^{**}P < 0.001$, $^{*}P < 0.05$. BDNF, brain-derived neurotrophic factor; CAMK, calcium calmodulin kinase; CREB, cyclic AMP response element-binding protein; ERK, extracellular signal-regulated kinase; SCR, scrambled RNA sequence; TRKB, Tropomyosin Receptor kinase B.

ischemic rats presented increased BDNF protein levels ($P < 0.001$; Figure 5A). This result was supported by an increase in levels of TRKB protein, which is the BDNF receptor ($P < 0.05$; Figure 5Ba, b). Additionally, the downstream activation of p-ser 133 CREB ($P < 0.05$; Figure 5Bc) and pERK1 ($P < 0.05$; Figure 5Ca) was increased in CDK5miR-treated ischemic animals compared with SCRmiR-treated ischemic animals (Figure 5C). pERK2, p-Thr 286-CAMKII (calcium calmodulin Kinase) and pSer473-Akt (also known as protein kinase B) were unmodified (Figure 5Cb–d).

DISCUSSION

The present study is the first to provide evidence that gene therapy based on CDK5 silencing during the acute phase of

ischemia/reperfusion accelerates sensorimotor recovery in the first week postischemia and prevents the occurrence of delayed cognitive impairment and neuropathologic hallmarks 1 month after ischemia.

Cyclin-dependent kinase 5 has a critical role in glutamate excitotoxicity after ischemia/reperfusion.[10,13] Its activity is associated with p25 and induces neuronal cell death, neuronal cytoskeleton breakdown, and hyperphosphorylation of the microtubule-associated protein tau.[27] Furthermore, transgenic mice that overexpress p25 via a neuron-specific promoter display severe axonal cytoskeleton disorganization and hyperphosphorylation of tau and neurofilament subunits.[28] The detrimental effects of p25/CDK5 activity have been explained by an accompanying deregulation of CDK5 activity due to the altered biologic properties of p25 compared with those of p35. p35 is rapidly degraded by ubiquitin-mediated proteolysis, resulting in a half-life of 20 to 30 minutes.[27] In contrast, p25 remains stable for a 5- to 10-fold longer duration, leading to a prolonged activation of Cdk5.[27]

Certain drugs, such as roscovitine or calpain inhibitors, that inhibit p25/CDK5 activity have been proposed as potential therapeutic tools for neuroprotection in stroke models. The systemic delivery of (S)-roscovitine, a well-known inhibitor of mitotic CDKs and CDK5, displays a dose-dependent neuroprotective effect in two models of focal ischemia.[10] TSNJ-1945 inhibits the calpain activation and protects against the effects of acute cerebral ischemia in mice, even when administered up to 6 hours after MCAO.[29] However, such pharmacological agents are not sufficiently specific and also appear to affect the physiologic function of CDK5 and/or the regulation of synaptic plasticity.[29] Therefore, their usage could lead to serious secondary side effects, thereby jeopardizing their therapeutic efficacy. In addition, to date, there is still no efficient mechanism for their safe delivery or the maintenance of their concentration at the injury site. Therefore, a particular strength of RNAi techniques is that they can be directed against specific gene targets.[14] Moreover, the use of adeno-associated viral vectors is advantageous because they are less immunogenic,[30] carry small sequences of DNA, and express the transgene for a longer period (up to 12 months after injection). Such vectors exhibit conserved silencing efficiency and effects on specific substrates, as we have verified in an Alzheimer's disease mouse model.[31]

Several studies have described the administration of siRNA against pathogenic genes involved in cerebral ischemia-induced apoptotic cell death and inflammation.[32] However, it is important to emphasize that in such studies, the siRNA was delivered before the ischemic event, restricting the translation of such a protocol into clinical practice. The relevance of the present study resides in that CDK5miR injection during ischemia/reperfusion produced the downregulation of CDK5 activity at 1 month after ischemia, as demonstrated by reduced CDK5 expression in the CA1 field region rostral to the injection site. Cyclin-dependent kinase 5 protein levels were unmodified in total hippocampal lysates, but lower levels of p25, CDK5 activity, and calpain activity were observed 1 month after ischemia. These results are very suggestive because calpain and p25 are necessary elements for CDK5 catalytic activation both *in vitro* and *in vivo*.[28]

The CDK5miR treatment protected the cerebral cortex from neurodegenerative events despite not being directly transduced into that ischemic tissue. This result was demonstrated by (1) sensorimotor score improvements during the first week after ischemia and (2) a significant reduction of the infarct volume and a decrease of CDK5 protein levels in the cerebral cortex and hippocampus 6 days after ischemia. Although, later was coincident with the intrinsic plasticity after ischemia recovery. Hippocampal CDK5 interference may somehow prevent the spread of excitotoxicity in the cortex. This result can most likely be explained by the central role of the hippocampus in regulating cortical plasticity.[33] Therefore, understanding of the circuitry underlying the regulatory role of the hippocampus in ischemia-induced cortical plasticity warrants further research. Additionally, our findings suggest that a direct CDK5miR injection into the ischemic cortex not only prevents penumbra damage but also would confer long-term protection against degenerative changes. Such effects could be useful for blocking progressive ischemia-induced impairments.

In addition, the delivery of CDK5miR during the ischemic event reduced the expression of neurodegeneration markers; blocked neuronal loss; inhibited cell death signaling by reducing Bax levels; prevented the expression of inflammation indicators, such as OX-42 and GFAP; and preserved MAP2 immunoreactivity and plasticity 1 month after tMCAO. Such findings were associated with the prevention of ischemia-induced cognitive deficits, such as difficulty to learn a spatial task, impairments with reversal learning of this task, and fragility of the associated memory trace. The protective effect of hippocampal CDK5 downregulation on spatial learning and memory implies an indirect protective effect on the neocortex, allowing the long-term storage of spatial information processed by the hippocampus.[34] In fact, the relearning of tasks have been described to be enhanced in CDK5 conditional knockout mice in which the expression of CDK5 is substantially reduced compared with that of wild-type animals.[35] Additionally, our group's previous studies have shown that CDK5 knockdown reduces phosphorylated tau levels, reduces neurofibrillary tangle number, and blocks rapid hippocampal neuronal loss in an elderly triple-transgenic mouse model of Alzheimer's disease,[17] possibly via p35/Rac1 signaling.[36] Moreover, such treatment improves spatial learning and memory function at 1 and 12 months after the injection.[31] These previous results most likely imply the regulation of phosphatases and other kinases, such as GSK3Beta. Another recent study showed that the selective inhibition of p25/CDK5 hyperactivation *in vivo* through overexpression of the CIP (CDK5 inhibitory peptide) rescues the neurodegenerative pathologies caused by p25/CDK5 hyperactivation without affecting normal neurodevelopment. Tau and amyloid pathologies as well as neuroinflammation are significantly reduced in CIP–p25 tetra transgenic mice. Brain atrophy and subsequent cognitive decline are also prevented in these animals.[37]

Interestingly, these previous behavioral findings were supported by CDK5 silencing-promoted hippocampal plasticity at 1 month after stroke in the present study. The CDK5miR treatment increased levels of BDNF, its TRKB receptor, and the downstream cascade proteins pCREB and pERK1. These results suggest that CDK5 downregulation, in an ischemia/reperfusion context, induces BDNF. This factor then leads to dendritic recovery, reduces of infarct volume, and increases neuronal connectivity and memory facilitation, in agreement with other studies.[38] Additionally, ERK1/2 is required for BDNF-induced increases in spine density on hippocampal pyramidal neurons and promotes memory.[39]

Finally, gene therapy using RNAi could be protective in the mid- and long-term after ischemic stroke and may offer a therapeutic option outside the gold standard therapeutic window of up to 4.5 hours.[40] In summary, based on our present results, silencing CDK5 seems to be a novel gene therapeutic strategy for reducing hallmark neuropathologic markers as well as the sensorimotor impairment and cognitive deficits associated with cerebral ischemia. Considering that stroke patients may relapse in successive ischemic episodes, with devastating long-term consequences, evaluating the effectiveness of such a therapeutic strategy when administered at different time windows after ischemia requires additional research.

DISCLOSURE/CONFLICT OF INTEREST

The authors declare no conflict of interest.

ACKNOWLEDGMENTS

The authors thank Dr Beverly Davidson and Dr Maria Scheel at the Viral Vector Core and Davidson Laboratory, University of Iowa, USA for viral vector expert advice.

REFERENCES

1 Moskowitz MA, Lo EH, Iadecola C. The science of stroke: mechanisms in search of treatments. *Neuron* 2010; **67**: 181–198.
2 Grotta J, Marler J. Intravenous rt-PA: a tenth anniversary reflection. *Surg Neurol* 2007; **68**: S12–S16.
3 Pan J, Konstas AA, Bateman B, Ortolano GA, Pile-Spellman J. Reperfusion injury following cerebral ischemia: pathophysiology, MR imaging, and potential therapies. *Neuroradiology* 2007; **49**: 93–102.
4 Chen RL, Balami JS, Esiri MM, Chen LK, Buchan AM. Ischemic stroke in the elderly: an overview of evidence. *Nat Rev Neurol* 2010; **6**: 256–265.
5 Aggarwal NT, Decarli C. Vascular dementia: emerging trends. *Semin Neurol* 2007; **27**: 66–77.
6 Wen Y, Yang S, Liu R, Simpkins JW. Transient cerebral ischemia induces site-specific hyperphosphorylation of tau protein. *Brain Res* 2004; **1022**: 30–38.
7 Barnett DG, Bibb JA. The role of Cdk5 in cognition and neuropsychiatric and neurological pathology. *Brain Res Bull* 2011; **85**: 9–13.
8 Dhavan R, Tsai LH. A decade of CDK5. *Nat Rev Mol Cell Biol* 2001; **2**: 749–759.
9 Fischer PM. Recent advances and new directions in the discovery and development of cyclin-dependent kinase inhibitors. *Curr Opin Drug Discov Devel* 2001; **4**: 623–634.
10 Menn B, Bach S, Blevins TL, Campbell M, Meijer L, Timsit S. Delayed treatment with systemic (S)-roscovitine provides neuroprotection and inhibits in vivo CDK5 activity increase in animal stroke models. *PLoS One* 2010; **5**: e12117.
11 Sielecki TM, Boylan JF, Benfield PA, Trainor GL. Cyclin-dependent kinase inhibitors: useful targets in cell cycle regulation. *J Med Chem* 2000; **43**: 1–18.
12 Glicksman MA, Cuny GD, Liu M, Dobson B, Auerbach K, Stein RL *et al.* New approaches to the discovery of cdk5 inhibitors. *Curr Alzheimer Res* 2007; **4**: 547–549.
13 Meyer DA, Torres-Altoro MI, Tan Z, Tozzi A, Di Filippo M, DiNapoli V *et al.* Ischemic stroke injury is mediated by aberrant Cdk5. *J Neurosci* 2014; **34**: 8259–8267.
14 Khvorova A, Reynolds A, Jayasena SD. Functional siRNAs and miRNAs exhibit strand bias. *Cell* 2003; **115**: 209–216.
15 Gonzalez-Alegre P. Therapeutic RNA interference for neurodegenerative diseases: From promise to progress. *Pharmacol Ther* 2007; **114**: 34–55.
16 Cespedes-Rubio A, Jurado FW, Cardona-Gomez GP. p120 catenin/alphaN-catenin are molecular targets in the neuroprotection and neuronal plasticity mediated by atorvastatin after focal cerebral ischemia. *J Neurosci Res* 2010; **88**: 3621–3634.
17 Piedrahita D, Hernandez I, Lopez-Tobon A, Fedorov D, Obara B, Manjunath BS *et al.* Silencing of CDK5 reduces neurofibrillary tangles in transgenic alzheimer's mice. *J Neurosci* 2010; **30**: 13966–13976.
18 Garcia JH, Wagner S, Liu KF, Hu XJ. Neurological deficit and extent of neuronal necrosis attributable to middle cerebral artery occlusion in rats. Statistical validation. *Stroke* 1995; **26**: 627–634.
19 Rivlin AS, Tator CH. Objective clinical assessment of motor function after experimental spinal cord injury in the rat. *J Neurosurg* 1977; **47**: 577–581.
20 Morris R. Developments of a water-maze procedure for studying spatial learning in the rat. *J Neurosci Methods* 1984; **11**: 47–60.
21 Joshi CN, Jain SK, Murthy PS. An optimized triphenyltetrazolium chloride method for identification of cerebral infarcts. *Brain Res Brain Res Protoc* 2004; **13**: 11–17.
22 Roulston CL, Callaway JK, Jarrott B, Woodman OL, Dusting GJ. Using behaviour to predict stroke severity in conscious rats: post-stroke treatment with 3', 4'-dihydroxyflavonol improves recovery. *Eur J Pharmacol* 2008; **584**: 100–110.
23 Gutierrez-Vargas JA, Munoz-Manco JI, Garcia-Segura LM, Cardona-Gomez GP. GluN2B N-methyl-D-aspartic acid receptor subunit mediates atorvastatin-Induced neuroprotection after focal cerebral ischemia. *J Neurosci Res* 2014; **92**: 1529–1548.
24 Johanna GV, Fredy CA, David VC, Natalia MV, Angel CR, Patricia CG. Rac1 activity changes are associated with neuronal pathology and spatial memory long-term recovery after global cerebral ischemia. *Neurochem Int* 2010; **57**: 762–773.
25 Sweatt JD. The neuronal MAP kinase cascade: a biochemical signal integration system subserving synaptic plasticity and memory. *J Neurochem* 2001; **76**: 1–10.
26 Hu Y, Russek SJ. BDNF and the diseased nervous system: a delicate balance between adaptive and pathological processes of gene regulation. *J Neurochem* 2008; **105**: 1–17.
27 Patrick GN, Zhou P, Kwon YT, Howley PM, Tsai LH. p35, the neuronal-specific activator of cyclin-dependent kinase 5 (Cdk5) is degraded by the ubiquitin-proteasome pathway. *J Biol Chem* 1998; **273**: 24057–24064.
28 Ahlijanian MK, Barrezueta NX, Williams RD, Jakowski A, Kowsz KP, McCarthy S *et al.* Hyperphosphorylated tau and neurofilament and cytoskeletal disruptions in mice overexpressing human p25, an activator of cdk5. *Proc Natl Acad Sci USA* 2000; **97**: 2910–2915.
29 Koumura A, Nonaka Y, Hyakkoku K, Oka T, Shimazawa M, Hozumi I *et al.* A novel calpain inhibitor, ((1S)-1((((1S)-1-benzyl-3-cyclopropylamino-2,3-di-oxopropyl) amino)carbonyl)-3-met hylbutyl) carbamic acid 5-methoxy-3-oxapentyl ester, protects neuronal cells from cerebral ischemia-induced damage in mice. *Neuroscience* 2008; **157**: 309–318.
30 Barros SA, Gollob JA. Safety profile of RNAi nanomedicines. *Adv Drug Deliv Rev* 2012; **64**: 1730–1737.
31 Castro-Alvarez JF, Uribe-Arias SA, Kosik KS, Cardona-Gomez GP. Long- and short-term CDK5 knockdown prevents spatial memory dysfunction and tau pathology of triple transgenic Alzheimer's mice. *Front Aging Neurosci* 2014; **6**: 243.
32 Zhang J, Wang Y, Zhu P, Wang X, Lv M, Feng H. siRNA-mediated silence of protease-activated receptor-1 minimizes ischemic injury of cerebral cortex through HSP70 and MAP2. *J Neurol Sci* 2012; **320**: 6–11.
33 Hosp JA, Luft AR. Cortical plasticity during motor learning and recovery after ischemic stroke. *Neural Plast* 2011; **2011**: 871296.
34 Nadel L, Hupbach A, Gomez R, Newman-Smith K. Memory formation, consolidation and transformation. *Neurosci Biobehav Rev* 2012; **36**: 1640–1645.
35 Hawasli AH, Benavides DR, Nguyen C, Kansy JW, Hayashi K, Chambon P *et al.* Cyclin-dependent kinase 5 governs learning and synaptic plasticity via control of NMDAR degradation. *Nat Neurosci* 2007; **10**: 880–886.
36 Posada-Duque RA, Lopez-Tobon A, Piedrahita D, Gonzalez-Billault C, Cardona-Gomez GP. p35 and Rac1 underlie the neuroprotection and cognitive improvement induced by CDK5 silencing. *J Neurochem* 201510.1111/jnc.13127.
37 Sundaram JR, Poore CP, Sulaimee NH, Pareek T, Asad AB, Rajkumar R *et al.* Specific inhibition of p25/Cdk5 activity by the Cdk5 inhibitory peptide reduces neurodegeneration in vivo. *J Neurosci* 2013; **33**: 334–343.
38 Chen A, Xiong LJ, Tong Y, Mao M. The neuroprotective roles of BDNF in hypoxic ischemic brain injury. *Biomed Rep* 2013; **1**: 167–176.
39 Alonso M, Medina JH, Pozzo-Miller L. ERK1/2 activation is necessary for BDNF to increase dendritic spine density in hippocampal CA1 pyramidal neurons. *Learn Mem* 2004; **11**: 172–178.
40 van der Worp HB, van Gijn J. Clinical practice. Acute ischemic stroke. *N Engl J Med* 2007; **357**: 572–579.